Stace, Thomas M.; Truong, Gar-Wing; Anstie, James D.; May, Eric F.; Luiten, André N. Power-dependent line-shape corrections for quantitative spectroscopy Physical Review A, 2012; 86(1):012506

http://link.aps.org/doi/10.1103/PhysRevA.86.012506

Power-dependent line-shape corrections for quantitative spectroscopy

Thomas M. Stace,[1] Gar-Wing Truong,[2] James Anstie,[2] Eric F. May,[3] and André N. Luiten[2,4]

[1]*ARC Centre for Engineered Quantum Systems, University of Queensland, St Lucia, Brisbane 4072, Australia*

[2]*Frequency Standards and Metrology Group, School of Physics, The University of Western Australia, 35 Hackett Drive, Crawley WA 6009, Australia*

[3]*Centre for Energy, School of Mechanical and Chemical Engineering, The University of Western Australia, 35 Hackett Drive, Crawley WA 6009, Australia*

[4]*School of Physics and Chemistry, The University of Adelaide, Adelaide, South Australia 5005, Australia*

(Received 20 February 2012; published 17 July 2012)

The Voigt profile—a convolution of a Gaussian and a Lorentzian—accurately describes the absorption lines of atomic and molecular gases at low probe powers. Fitting experimental absorption data to such a Voigt profile yields both the Lorentzian natural linewidth and the Gaussian Doppler broadening. However, as the probe power increases, saturation effects change the absorption line shape, such that it is no longer accurately described by a Voigt profile. Naively fitting a simple Voigt profile to the absorption line therefore introduces spurious power dependence into the extracted Doppler component. Using a simple atomic model, we calculate power-dependent corrections to the Voigt profile, which are parametrized by the Gaussian Doppler width, the Lorentzian natural linewidth, and the optical depth. We show numerically and experimentally that including the correction term substantially reduces the spurious power dependence in the fitted Gaussian width.

DOI: 10.1103/PhysRevA.86.012506 PACS number(s): 32.30.−r, 07.20.Dt, 82.80.Dx

I. INTRODUCTION

Vapor cell spectroscopy is important for determining the properties of atomic or molecular transitions [1,2]. Spectral absorption line shapes can usually be well described by the workhorse of spectroscopy: the Voigt profile. Experimental progress has reached the point that intensity-dependent corrections to the Voigt profile are becoming significant. For example, molecular fingerprinting and other trace gas measurement applications [3,4] using direct frequency comb spectroscopy (DFCS) [5] require a quantitative link between absorption depths and gas concentrations, particularly if the probe laser intensity levels are increased to improve signal-to-noise in challenging environments. While absorption sensitivities measured using DFCS can be determined with quantum-noise limited precision [6,7], the effects of optical pumping on the observed depths and line shapes remain to be quantified. Similar issues are faced in the use of spectroscopy to determine Boltzmann constant k_B from measurements of Doppler-broadened line shapes [8–14]. To optimize the trade-off between signal-to-noise limitations at very low powers, and systematic optical pumping effects at higher powers, an accurate theory of the line-shape dependence on probe intensity is essential.

In the limit of low probe powers, where atomic populations are hardly perturbed from their thermodynamic equilibrium values, transmission spectra are well described by a Voigt profile [15,16], $\mathcal{T}_{\rm lin}(z) = e^{-Kz V_\nu(\Delta)}$, where K is the absorptivity, z is the length of the vapor cell, Δ is the detuning from resonance (note that all times and frequencies are expressed in units of $\Gamma = \Gamma_{\rm natural}/2$), $\nu = \gamma/\Gamma$ is the Doppler width γ, normalized Γ, and V is a convolution of a Gaussian and a Lorentzian:

$$V_\nu(\Delta) \equiv \frac{1}{\pi^{3/2}\nu}\int_{-\infty}^{\infty}\frac{e^{-(x-\Delta)^2/\nu^2}}{1+x^2}\,dx,$$
$$= \mathrm{Re}\{e^{-(i+\Delta)^2/\nu^2}\mathrm{erfc}[-i(i+\Delta)/\nu]/(\sqrt{\pi}\nu)\},$$

where $\mathrm{erfc}(z) = 2\int_z^\infty e^{-t^2}dt/\sqrt{\pi}$.

At low probe powers, $\mathcal{T}_{\rm lin}$ describes the measured transmission spectrum very accurately; the Gaussian component arises from the Doppler shifts due to the atomic Maxwell-Boltzmann velocity distribution, while the Lorentzian relates to atomic relaxation processes. Fitting $\mathcal{T}_{\rm lin}$ to experimental measurements yields γ, Γ, and the optical depth. However, as the probe power increases, perturbations away from the thermal-equilibrium atomic population distribution become significant and $\mathcal{T}_{\rm lin}$ fails to accurately represent the transmission spectrum. In the limit of large probe powers, atomic populations depart from the values at thermodynamic equilibrium: In two-level atoms the ground and excited states tend to equalize; in three-level systems population may be transferred to an optically inactive state. In either case, fitting $\mathcal{T}_{\rm lin}$ to the measured spectrum yields incorrect values for γ and Γ, which acquire a spurious intensity dependence.

In this paper, we derive the intensity-dependent corrections to $\mathcal{T}_{\rm lin}$, which can be computed perturbatively in powers of the laser intensity. We then show, both theoretically and experimentally, that fitting to the corrected form yields Doppler widths that are independent of intensity as they should be. This result will enable accurate measurements of Doppler broadening in quantitative spectroscopy at much higher probe intensities, where saturation effects are not negligible. This in turn greatly enhances the signal-to-noise ratio in a given integration time.

We begin by computing the spectral dependence on the atomic populations for a three-level atom, consisting of two ground states: one optically active, $|1\rangle$, and the other optically inactive, $|2\rangle$, and an excited state $|3\rangle$, as discussed in Ref. [17]. Transitions between states $|1\rangle$ and $|3\rangle$ are optically driven, and state $|3\rangle$ can relax to either of the ground states. Recalling that all times and frequencies are denoted in units of $\Gamma = \Gamma_{\rm natural}/2$, the population rate equations are

$$\dot{\vec{P}} = M\vec{P}, \quad M = \begin{pmatrix} \frac{\Omega^2 f(t)/2}{1+\Delta^2} & 0 & 2\beta + \frac{\Omega^2 f(t)/2}{1+\Delta^2} \\ 0 & 0 & 2(1-\beta) \\ -\frac{\Omega^2 f(t)/2}{1+\Delta^2} & 0 & -2 - \frac{\Omega^2 f(t)/2}{1+\Delta^2} \end{pmatrix}, \quad (1)$$

where $\vec{P} = \{P_1, P_2, P_3\}$, Δ is the detuning between the laser frequency and the atomic transition, β is the branching ratio from state $|3\rangle$ to $|1\rangle$, Ω is a characteristic size of the atomic Rabi frequency (proportional to the electric field amplitude), and $\sqrt{f(t)}$ represents the temporal profile of the Rabi frequency experienced by the atom as it moves through regions of different intensity. We write the Rabi frequency in this form since in what follows we will expand the atomic response in powers of $\Omega^2/(1+\Delta^2)$. For simplicity of presentation, we will assume that the equilibrium atomic level populations are $\vec{P}_{\rm eq} = \{1/2, 1/2, 0\}$ (i.e., we ignore degeneracies in the ground-state manifold). Accounting for degeneracies is a simple modification to the relative fractions for P_1 and P_2 at equilibrium.

The three-level model described above is sufficiently generic to calculate the line-shape and intensity-dependent corrections thereto: a multiplicity of optically inactive states would simply be accounted for by defining P_2 to be the population of these states collectively, while degeneracy in the optically active transition modifies the equilibrium populations, which appears as an overall scale factor in the absolute absorption.

The light is absorbed as it propagates through the atomic medium, and the axial evolution of the field is governed by Ref. [17]

$$\frac{\partial \ln \Omega^2}{\partial z} = 2K \int_{-\infty}^{\infty} d\Delta_{v_z} \frac{e^{-(\Delta-\Delta_{v_z})^2/v^2}}{1+\Delta_{v_z}^2} P(\Delta_{v_z}), \qquad (2)$$

where $P = P_3 - P_1$, $K = \rho_0 \mu^2/(\sqrt{\pi}\varepsilon_0 \hbar v_0)$, μ is the transition dipole moment, and $v_0 = \sqrt{2k_B T/m}$ is the mean thermal atomic velocity for an atom of mass m. The notation Δ_{v_z} indicates that a given atom is subject to a detuning which depends on its axial velocity via the Doppler shift. If the field intensity is weak, so that on resonance populations are negligibly perturbed from thermal equilibrium, then $P = -1/2$, and the integral yields $\Omega^2(z) = \Omega_0^2 e^{K z V_v(\Delta)}$. Since $\mathcal{T}(z) = \Omega^2(z)/\Omega_0^2$, we recover $\mathcal{T} = \mathcal{T}_{\rm lin}$.

As Ω^2 grows, perturbations to P become significant, and we need to compute corrections to P arising from the dynamics described by Eq. (1). Since we are concerned with small but significant pump-induced perturbations to the thermal population, we do a perturbative analysis of Eq. (1) around the limiting case where $\Omega = 0$.

II. CORRECTIONS TO VOIGT PROFILE

We can easily guess the form of the $O(\Omega^2)$ correction to the population difference P: By inspection of Eq. (1) we see that Ω^2 only ever appears as part of the ratio $\Omega^2/(1+\Delta^2)$, so it must appear in the same ratio in P, that is, we anticipate that

$$P(\Delta) = -\frac{1}{2} + q\,\frac{\Omega^2}{1+\Delta^2} + O\left(\left(\frac{\Omega^2}{1+\Delta^2}\right)^2\right), \qquad (3)$$

where q is some as yet undetermined expansion coefficient.

To see this formally, we write $M = M_0 + f(t)\frac{\Omega^2}{1+\Delta^2} M_1$ where

$$M_0 = \begin{pmatrix} 0 & 0 & 2\beta \\ 0 & 0 & 2(1-\beta) \\ 0 & 0 & -2 \end{pmatrix}, \quad M_1 = \begin{pmatrix} \frac{1}{2} & 0 & \frac{1}{2} \\ 0 & 0 & 0 \\ -\frac{1}{2} & 0 & -\frac{1}{2} \end{pmatrix}. \qquad (4)$$

We define $\vec{Q}(t)$ such that $\vec{P}(t) = e^{M_0 t}\vec{Q}(t)$. Substituting this expression into Eq. (1) yields a new set of equations for $\vec{Q}(t)$:

$$\dot{\vec{Q}} = \frac{\Omega^2}{1+\Delta^2} \tilde{M}_1(t)\,\vec{Q}, \qquad (5)$$

where $\tilde{M}_1(t) = f(t) e^{-M_0 t} M_1 e^{M_0 t}$. The formal solution to Eq. (5) can be written as a time-ordered product, from which the solution for $P(t)$ is

$$\begin{aligned} \vec{P}(t) &= e^{M_0 t} \mathsf{T} e^{\frac{\Omega^2}{1+\Delta^2}\int_{-\infty}^{t} d\tau \tilde{M}_1(\tau)} \vec{P}_{\rm eq}, \\ &= e^{M_0 t}\left(1 + \frac{\Omega^2}{1+\Delta^2}\int_{-\infty}^{t} d\tau \tilde{M}_1(\tau) + \cdots\right)\vec{P}_{\rm eq}, \end{aligned} \qquad (6)$$

where T denotes the time-ordered product, and $\vec{P}_{\rm eq}$ is the thermal equilibrium distribution of atomic level populations. In the second line, we have expanded the time-ordered matrix exponential to first order in Ω^2, dropping higher order terms. We note that $e^{M_0 t}$ acts as the identity on the ground-state manifold, and since the thermal occupation of level $|3\rangle$ is essentially zero, we see that $e^{M_0 t}\vec{P}_{\rm eq} = \vec{P}_{\rm eq}$ (i.e., the zeroth-order solution is to leave the equilibrium populations unaltered, as expected). Substituting P_1 and P_3 from Eq. (6) into the population difference $P(\Delta_{v_z}) = P_3(\Delta_{v_z}) - P_1(\Delta_{v_z})$ we recover Eq. (3) where

$$q = \int_{-\infty}^{t} d\tau(\beta - (\beta+1)e^{2(\tau-t)} - 1) f(\tau)/4.$$

In the simple case where $f(\tau)$ is a top-hat function (unity for $0 < \tau < t$ and zero otherwise), we find $q \approx (1+\beta+2t(1-\beta))/8$.

Substituting Eq. (3) into Eq. (2) yields

$$\frac{\partial \ln \Omega^2}{\partial z} = -K\,V_v(\Delta) + K\,q\,V_v^{(2)}(\Delta)\,\Omega^2 + O(\Omega^4), \qquad (7)$$

where

$$V_v^{(n)}(\Delta) = \int_{-\infty}^{\infty} d\Delta_{v_z} \frac{e^{-(\Delta-\Delta_{v_z})^2/v^2}}{\left(1+\Delta_{v_z}^2\right)^n}$$

is a generalization of the Voigt profile.

$V^{(2)}$ may be evaluated by noting that

$$\frac{1}{(1+x^2)^2} = \lim_{a\to 1}\left\{\frac{a^2}{(a^2-1)(a^2x^2+1)} + \frac{1}{(1-a^2)(x^2+1)}\right\}.$$

Convolving this sum of two Lorentzians with a Gaussian thus yields a sum of Voigt functions,

$$\begin{aligned} V_v^{(2)}(\Delta) &= \lim_{a\to 1}\left\{\frac{a^2}{(a^2-1)} V_{a\,v}(a\,\Delta) + \frac{1}{(1-a^2)} V_v(\Delta)\right\} \\ &= \mathrm{Re}\left\{\frac{v + \sqrt{\pi} e^{-\frac{(\Delta+i)^2}{v^2}}(i\Delta + v^2/2 - 1)\mathrm{erfc}(\frac{1-i\Delta}{v})}{\pi v^3}\right\}. \end{aligned}$$

Higher order correction terms can be calculated iteratively, using the same method.

Equation (7) can be solved analytically to give

$$\mathcal{T} = \frac{e^{-K z V_v(\Delta)}}{1 + q\,\Omega_0^2\,V_v^{(2)}(\Delta)(e^{-K z V_v(\Delta)} - 1)/V_v(\Delta)}. \qquad (8)$$

Expanding this expression, and recalling that all quantities are nondimensionalized in units of Γ we explicitly include the Lorentz width as a parameter:

$$\mathcal{T} \approx e^{\tilde{p} V_\nu(\Delta/\Gamma)+\tilde{q}(e^{\tilde{p} V_\nu(\Delta/\Gamma)}-1)\, V_\nu^{(2)}(\Delta/\Gamma)/V_\nu(\Delta/\Gamma)}, \qquad (9)$$

where $\tilde{p} = -K\, z$ and $\tilde{q} = -q\, \Omega_0^2$. This correction, linear in $\tilde{q} \propto I$, is the central result of this paper. If either the intensity ($\propto \tilde{q}$) is small, or if the optical depth ($\propto \tilde{p}$) is small, the correction vanishes and the well-known Voigt profile is recovered. In the latter case, saturation effects may be substantial, however, the optical depth of the sample is sufficiently short that only a small fraction of incident photons are absorbed. In what follows we demonstrate both numerically and experimentally the advantages of using Eq. (9) when fitting spectra for which saturation effects become significant.

We note that because Eqs. (3) and (7) are valid for any time-dependent intensity profile that a given atom experiences, it follows that the form of the correction term in Eq. (9) is correct for any temporal intensity profile that a given atom experiences. Indeed, since different atoms follow different trajectories through the beam, and do so at different speeds, the atomic ensemble will sample from some distribution of q's. However, since the right-hand side of Eq. (7) is linear in q, when we average over this distribution, we simply replace q in Eq. (7) with the distribution average $\bar{q}$. Then both the complicated time dependence in q, and the distribution of different q's are simply absorbed into the parameter $\tilde{q}$. The consequence of this is that Eq. (9) is the physically correct form to account for linear power-dependent corrections to the Voigt profile.

A typical Voigt profile and the correction are shown in Fig. 1. In fitting to spectra, ν, $\tilde{p}$, and $\tilde{q}$ are treated as fitting parameters.

We also numerically investigate leaving the decay rate Γ as a free-fitting parameter. We emphasize that this is an *ad hoc* modification, since the analysis above treats Γ as a known atomic quantity. However, higher order intensity-dependent terms, which we have neglected, contribute additional broadening to the spectrum, so allowing Γ to vary is a heuristic way of accounting for nonlinear intensity-dependent broadening. In what follows, we demonstrate that in practice it yields a modest improvement in the accuracy of the returned Doppler width.

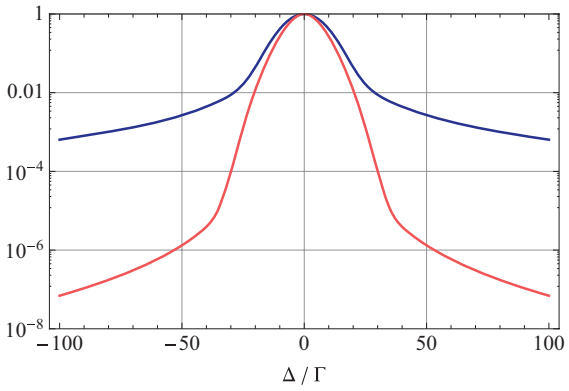

FIG. 1. (Color online) Typical form for the Voigt function (dark, blue), and the correction term multiplying $\tilde{q}$ in Eq. (9) (light, red), for $\nu = 10, \tilde{p} = 20$.

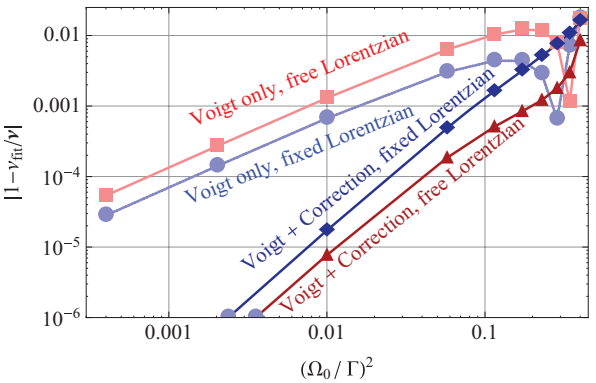

FIG. 2. (Color online) Fits to numerically simulated spectra, showing the fractional error in the extracted, normalized Doppler width as a function of normalized probe intensity for different fitting functions. (Solid squares and circles) Voigt-only fits; (solid diamonds and triangles) include the correction term. (Solid squares and triangles) We also allow the Lorentzian width to vary.

III. NUMERICAL TEST OF VOIGT CORRECTION

To evaluate the efficacy of the correction, we numerically simulate an absorption spectrum using Eq. (2) [keeping terms in P up to $O(\Omega^6)$], and then attempt to extract the simulation parameters by fitting Eq. (9). For comparison, we compare fits with Voigt only ($\tilde{q} = 0$) and Voigt plus correction ($\tilde{q}$ free); in combination with a fixed Lorentzian ($\Gamma = 0$) and free Lorentzian (Γ free). Figure 2 shows the deviation of $\nu_{\rm fit} = \gamma_{\rm fit}/\Gamma$ from the correct value ν, as a function of intensity ($\propto (\Omega_0/\Gamma)^2$) for the different fitting forms. As expected, all fitting forms yield the correct value for $\nu_{\rm fit}$ as $\Omega_0^2 \to 0$. Without the correction (solid squares and circles), the fit converges to the correct value as Ω_0^2. This improves to Ω_0^4 when the correction is included (solid diamonds and triangles).

The fitting performance is further illustrated in Fig. 3 (left), which shows the dependence of the fitted parameters $\nu_{\rm fit}/\nu$ (top) and Γ (bottom) as a function of the probe intensity ($\propto(\Omega_0/\Gamma)^2$, for a particular representative choice of parameters ($\beta = 1/2$, $t = 20$, $\nu = 100$). Also shown is the fitted Lorentzian component [Fig. 3 (bottom)], demonstrating apparent broadening of the atomic lifetime, even for intensities substantially below the saturation intensity. This phenomenon has been observed experimentally [7].

Qualitatively, at low powers the uncorrected, Voigt-only fits (solid squares and circles) systematically underestimate ν over a range of laser powers, and demonstrate a pronounced minimum, as illustrated in Fig. 3 (top). In the case where the Lorentzian is held fixed (solid circles), the Voigt-only fit may over- or underestimate the Doppler width, depending on the parameters (i.e., the initial slope may be positive or negative). For the parameter choices in the simulated spectra [Fig. 3 (left)], the initial slope is slightly negative, and there is a noticeable minimum in $\nu_{\rm fit}/\nu$.

We note that since Eq. (9) is the result of a perturbative expansion in $(\Omega_0/\Gamma)^2$, we expect it to break down at large powers, in particular when $\Omega_0/\Gamma \lesssim 1$. This is evident at the

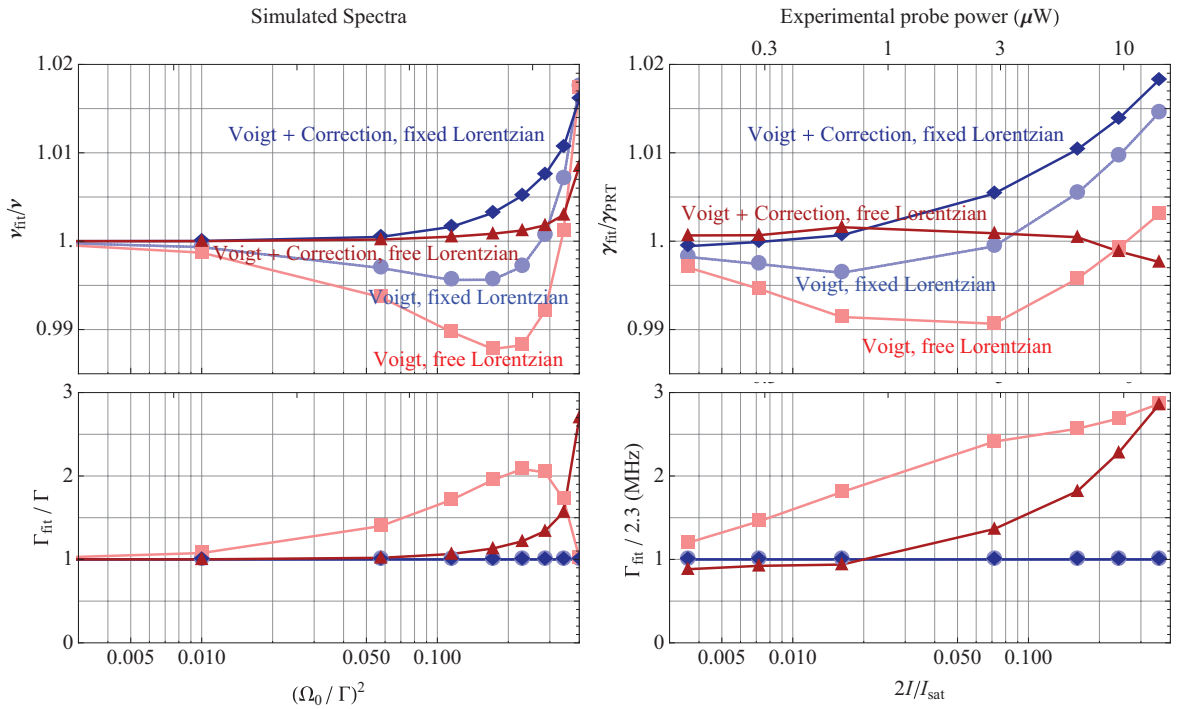

FIG. 3. (Color online) Fits to (left) simulated data using Eq. (2), with $\beta = 1/2$, $t = 20$, $\nu = 100$; (right) experimental data taken from Ref. [7]. (Top) Fitted Doppler widths, extracted from fits to Voigt only or Voigt plus correction, with fixed or free Lorentzian widths. (Bottom) Fitted Lorentzian widths, normalized to the natural linewidth.

right-hand side of each panel of Fig. 3, where the extracted Doppler and natural line widths diverge from the correct values.

IV. EXPERIMENTAL TEST OF VOIGT CORRECTION

We now demonstrate the effectiveness of using the corrected transmission function for extracting the true atomic velocity distribution from experimental data. Spectra from the cesium D_1 transition were recorded in a 7-cm-long vapor cell (no buffer gas) at approximately 295 K at different probe powers, using a collimated 2-mm-diameter laser. At this temperature, the mean free path is several meters, so collisional effects are negligible. At each power setting, 16 spectral scans were taken, and each scan was fitted using Eq. (9) to yield estimates for $\gamma_{\rm fit}$ and $\Gamma_{\rm fit}$. For each scan, the temperature was recorded using a platinum resistance thermometer (PRT), calibrated for thermometry to ± 100 ppm. Each fitted Doppler width $\gamma_{\rm fit}$ was normalized by the width expected given the temperature measured using the PRT, $\gamma_{\rm PRT} = \omega_{\rm probe}\sqrt{2k_B T_{\rm PRT}/m}/c$, where $\omega_{\rm probe}$ is the frequency of the probe laser.

To qualitatively compare the fitting results from the simulated spectra with the experimental results, we convert the laser power to an average intensity by dividing the power by the beam area, $\pi(1\ {\rm mm})^2$, and then normalize this average intensity by the saturation intensity $I_{\rm sat} = 2.51\ {\rm mW/cm^2}$ [18], so that the nondimensional experimental parameter, $2I/I_{\rm sat}$, is equivalent to the nondimensional simulation parameter $(\Omega/\Gamma)^2$.

The results are shown in Fig. 3 (right). For $2I/I_{\rm sat} < 0.1$, the extracted Doppler widths are substantially better when using the correction than not, as shown in Fig. 3 (right, top). This is in qualitative agreement with the simulated data. For the lowest powers used, the corrected estimates for the Doppler width are at least an order of magnitude better than the uncorrected form, limited by the accuracy of the PRT calibration, and statistical uncertainty from the small sample size.

V. DISCUSSION AND CONCLUSIONS

Comparing Fig. 3 (left and right) shows that the simulated results are in qualitative agreement with the experimentally derived results in other respects as well, including the relative locations of minima, slopes, and crossing points. Quantitative differences arise from the simplified physical model underpinning the simulated spectra, in which the distribution of atomic crossing times and intensity profiles is replaced by the average crossing time and the average intensity. While not unphysical, this differs from the experimental conditions.

In thermometry, where the objective is to extract very accurate Doppler widths from spectral data, we see from Fig. 2 that it is important to use the Voigt correction. For instance, if $2I/I_{\rm sat} \sim 0.003$ then a fit to a Voigt-only profile has a systematic bias in the fitted Doppler width at the level of nearly 10^3 ppm. In contrast, using the corrected form yields an estimate of the Doppler width that is accurate to $\sim$1 ppm, which is comparable to the current thermometric state of the art.

It follows that under the comparable experimental conditions represented in Fig. 3 (right), to reduce the systematic

bias in the fitted Doppler width to 1 ppm (when utilizing the corrected form), the probe beam should operate at $2I/I_{\text{sat}} = 0.003$, corresponding to a laser power of 100 nW in a 2-mm-diameter beam.

One important application of Doppler spectroscopy is to contribute to the CODATA redefinition of Boltzmann's constant [9,10,13,14], in which the vapor cell is at equilibrium with a triple-point-of-water reference at 273.16 K. At this temperature the optical depth of the cell is ∼10 times smaller than under the experimental conditions reported here. As such, the intensity may be increased by the same factor, to ∼1 μW, while still maintaining the systematic Doppler error at ∼1 ppm.

In conclusion, we have derived the power-dependent correction to the Voigt profile, and demonstrated numerically and experimentally that including the correction term yields much better estimates of the width of the underlying Gaussian process, substantially reducing the spurious power dependencies that arise from an uncorrected Voigt profile. We anticipate that this will find direct application in the near-term to high-precision spectroscopy and thermometry of atomic vapor cells.

[1] B. Sherlock and I. Hughes, Am. J. Phys. **77**, 111 (2009).

[2] M. L. Harris, C. S. Adams, S. L. Cornish, I. C. McLeod, E. Tarleton, and I. G. Hughes, Phys. Rev. A **73**, 062509 (2006).

[3] M. Thorpe, D. Balslev-Clausen, M. Kirchner, and J. Ye, Opt. Express **16**, 2387 (2008).

[4] F. Adler, M. Thorpe, K. Cossel, and J. Ye, Annual Review of Analytical Chemistry **3**, 175 (2010).

[5] S. Diddams, L. Hollberg, and V. Mbele, Nature (London) **445**, 627 (2007).

[6] A. Foltynowicz, T. Ban, P. Masłowski, F. Adler, and J. Ye, Phys. Rev. Lett. **107**, 233002 (2011).

[7] G.-W. Truong, J. D. Anstie, A. N. Luiten, E. May, and T. M. Stace, arXiv:1203.3338v1.

[8] G. W. Truong, E. F. May, T. M. Stace, and A. N. Luiten, Phys. Rev. A **83**, 033805 (2011).

[9] G. Casa, A. Castrillo, G. Galzerano, R. Wehr, A. Merlone, D. Di Serafino, P. Laporta, and L. Gianfrani, Phys. Rev. Lett. **100**, 200801 (2008).

[10] C. Daussy, M. Guinet, A. Amy-Klein, K. Djerroud, Y. Hermier, S. Briaudeau, C. J. Bordé, and C. Chardonnet, Phys. Rev. Lett. **98**, 250801 (2007).

[11] P. Mohr and B. Taylor, Rev. Mod. Phys. **77**, 1 (2005).

[12] C. Bordé, Phil. Trans. Roy. Soc. A **363**, 2177 (2005).

[13] K. Djerroud, C. Lemarchand, A. Gauguet, C. Daussy, S. Briaudeau, B. Darquié, O. Lopez, A. Amy-Klein, C. Chardonnet, and C. Bordé, Comptes Rendus Physique **10**, 883 (2009).

[14] A. Castrillo, G. Casa, A. Merlone, G. Galzerano, P. Laporta, and L. Gianfrani, Comptes Rendus Physique **10**, 894 (2009).

[15] W. Demtröder, *Laser Spectroscopy: Basic Concepts and Instrumentation* (Springer, Berlin, 1981).

[16] C. Bordé, Comptes Rendus Physique **10**, 866 (2009).

[17] T. M. Stace and A. N. Luiten, Phys. Rev. A **81**, 033848 (2010).

[18] D. Steck, *Cesium D Line Data* [http://steck.us/alkalidata] (2003).